

## Dynamic behaviour of speckle cluster formation

A. LENCINA<sup>†</sup>, M. TEBALDI <sup>‡</sup>, P. VAVELIUK<sup>§</sup> and N. BOLOGNINI<sup>¶</sup>

<sup>†</sup>Centro de Investigaciones Ópticas (CONICET-CIC), La Plata, Argentina

<sup>‡</sup>Centro de Investigaciones Ópticas (CONICET-CIC) and UID OPTIMO, Facultad de Ingeniería, Universidad Nacional de La Plata, La Plata, Argentina. PO Box 124, La Plata (1900), Argentina

<sup>§</sup>Departamento de Física, Universidade Estadual de Feira de Santana, Campus Universitário, BR116, KM 03, Feira de Santana 44031-460, Bahia, Brazil

<sup>¶</sup>Centro de Investigaciones Ópticas (CONICET-CIC) and UID OPTIMO, Facultad de Ingeniería, Universidad Nacional de La Plata and Facultad de Ciencias Exactas, Universidad Nacional de La Plata, PO Box 124, La Plata (1900), Argentina

In this work, we analyse the speckle cluster structure generated when a coherently illuminated diffuser is imaged by introducing a multiple aperture pupil mask in front of the lens plane. We demonstrate that the speckle cluster originates from the complex speckle modulation generated by multiple interferences among the wavefront passing through each aperture. The auto-correlation function of the intensity distribution when using a multiple aperture pupil arrangement is calculated. Besides, we demonstrate that the autocorrelation function and the intensity corresponding to a single scattering element of the input are coincident. This result allows interpretation of the dynamics behaviour of the speckle cluster formation by considering the result obtained by a single scattering element. Then, we determine the pupil mask geometrical parameters that control the cluster behaviour and therefore the condition for obtaining a highly repetitive cluster structure that we define as a 'regular cluster'. The theoretical simulations based on the random walk model are in agreement with the experimental results supporting the validity of our approach.

### 1. Introduction

It is well known that the multiple interference among the wavefront scattered from each element of a diffuser object illuminated by coherent light generates a speckle pattern. The diffuser can be considered as an ensemble of scattering elements with random distributions of phase, position and shape. Speckle patterns are obtained either by using an imaging formation system or by free propagation, usually defined as subjective or objective speckles, respectively [1, 2]. The internal modulation of the speckle achieved by locating a multiple aperture pupil mask in front of the imaging lens allows the implementation of several metrological methods [3–8]. Applications using multiple aperture pupils demonstrate the possibility of carrying out a variety of experiments that cannot be implemented otherwise. For instance, optical arrangements for image multiplexing [3], speckle photography [4, 5] and speckle interferometry [6–8] have been proposed.

---

In an early work, Uno *et al.* [9] showed that when a rough surface is illuminated with a ring-slit aperture, a speckle pattern formed in its Fraunhofer diffraction region presents a string or network-like structure appearance, which is called speckle clustering. In this work, the authors stated that speckle clusters suggest the existence of a longer correlation beyond the speckle size. It was shown that the speckle clustering phenomenon can be explained by long ringing lobes that are present in the autocorrelation function of the speckle pattern generated with ring-slit illumination. In [10], the speckle pattern from ring slit illumination was compared with other types of illumination (segmented ring-slit apertures). Also, it was found that the speckle has a clustering appearance with a characteristic spatial structure.

In our proposal, we study the subjective speckle behaviour when a plane wave illuminates an input diffuser and a ring-slit aperture pupil is attached to the imaging lens. Although our set-up differs from the arrangement proposed in [9, 10], the intensity distributions obtained in the image plane replicate the characteristic spatial structures as observed in [10]. Therefore, we maintain for those intensity distributions the ‘cluster’ terminology. It should be mentioned that a ring-slit aperture could be represented as a continuous arrangement of apertures distributed on a circumference. Then, we use the multiple apertures scheme analysed in [11, 12] to interpret the speckle cluster generation. We found that by using the mentioned scheme the speckle image distributions have cluster structures with remarkable regularity. This behaviour was not previously observed. This new feature motivates us to develop a deeper systematic analysis of the cluster structures. The experimental results confirmed by the theoretical analysis demonstrate that the cluster structure is a consequence of the internal speckle modulations generated by the multiple interference produced by the aperture pupil. Indeed, directional structures appear in the inner speckle modulation so that tiny spots are found on regular arrangements that replicate the aperture distribution in the pupil. We define this particular structure as a ‘regular cluster’. In fact, this assertion implies that we are able to generate highly localized three-dimensional intensity patterns. On the other hand, let us remember that optical micromanipulation requires novel light beams to operate and to trap microscopic particles. This idea suggests that the cluster structures could be useful for tweezing several particles at once, due to their high directional nature.

In our work, we demonstrate that the image intensity distribution corresponding to a single scattering element in the input plane is equivalent to the auto-correlation function. This result is the starting point for interpreting the speckle cluster formation. Afterwards, we demonstrate that the regular cluster formation depends on the following parameters: the number of apertures  $N$ , the radius of the apertures  $R$ , the uniformity of the distribution of the apertures and the circumference radius  $r$  of the distribution of the apertures. We confirm this fact through the agreement between the experimental results and the theoretical simulations obtained by using the random walk model [12].

## 2. Experimental description

The experimental set-up is shown in figure 1. The results of this section are obtained using an expanded and collimated beam provided by a linearly polarized mini Nd YAG laser ( $\lambda = 532$  nm). Our scheme is a subjective speckle arrangement. In this case, a singlet lens  $L$  image in the  $X - Y$  plane with a random diffuser  $D$ . The scattering element  $D$  located in the  $X - Y$  plane is a  $30 \mu\text{m}$  rms glass diffuser. The focal length of the lens  $L$  located in the  $U - V$  plane is 52 mm. The distances from the diffuser to the lens  $Z_0$  and from the lens to the image plane  $Z_C$  are 56 mm and 717 mm, respectively. A pupil mask  $P$  is located immediately in front of the imaging lens  $L$ . The experimental speckle images are recorded by using a CCD camera

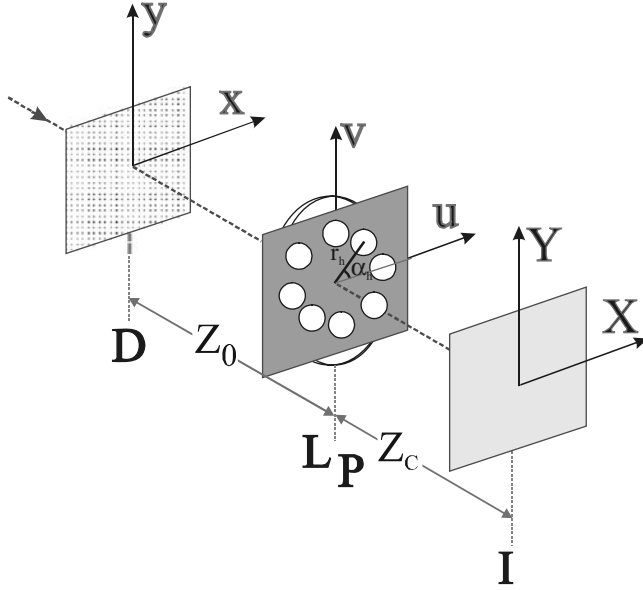


Figure 1. Experimental set-up:  $D$ , diffuser;  $L$ , imaging lens;  $P$ , pupil mask;  $I$ , image plane.

with a zoom-microscope focused on the observation  $X - Y$  plane. The area in the object plane in the experimental and simulated results is  $0.7 \text{ mm} \times 1.2 \text{ mm}$ . This area corresponds in the diffuser plane to an area of about  $55 \mu\text{m} \times 94 \mu\text{m}$ .

Figure 2 shows the experimental image speckle pattern corresponding to a continuous ring-slit pupil obtained using the set-up in figure 1. A cluster structure with a network-like appearance is clearly observed. This result resembles that obtained in [9, 10].

Note that it is valid to represent a circular ring slit as an arrangement of discrete apertures distributed on a circumference that resembles the continuous ring slit. Then, we consider a pupil mask consisting of  $N$  identical circular apertures  $a_1, a_2 \dots a_N$  of radius  $R$  distributed in a circumference of radius  $r$ .

Figure 3 shows the speckle pattern corresponding to 16 apertures uniformly distributed in a circumference. In this case, a cluster structure also appears in the image. A comparison of figures 2 and 3 shows that in the discrete case the image exhibits a more regular cluster structure. This fact encourages further analysis to determine the conditions that improve or do not improve the regularity that the cluster structure presents.

### 3. Theoretical discussion

In the following, we discuss a model to interpret the dynamic behaviour of cluster formation. Let us remember that when utilizing a multiple aperture pupil, each aperture forms a speckled image of the diffuser. Besides, the complex amplitudes of waves going through different apertures are statistically independent, because different components of the angular spectrum of the scattered light are accepted by them. Moreover, the resulting speckle pattern appears as the interference of speckle distributions produced by each aperture pair because they are coherent. In summary, a complex system of fringes existing in the whole volume of each individual speckle modulates the resulting speckle pattern.

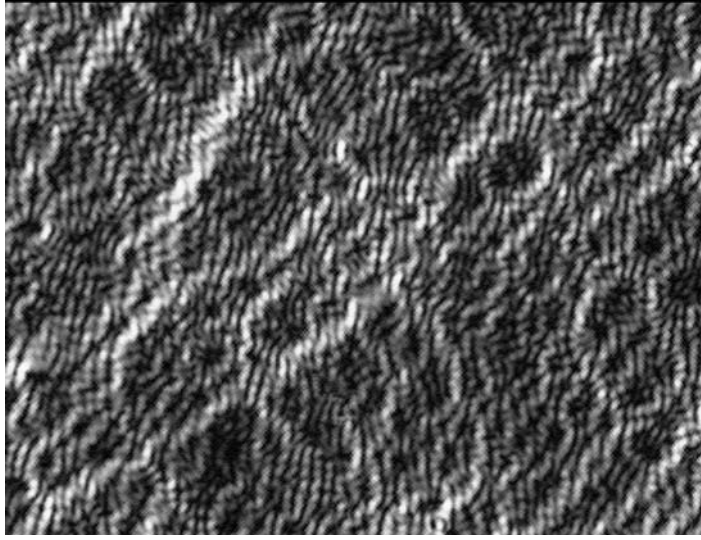


Figure 2. Experimental speckle pattern corresponding to a continuous ring-slit pupil.

### 3.1 *Random walk model*

An approach is introduced [12] to describe the resulting subjective speckle pattern when a generic multiple aperture pupil is used. This approach is based on the random walk model and a new approximation for the quadratic phase factors is given. In the double aperture pupil case, the theoretical calculations presented in [12] fully coincide with the experimental results. Then, the model proposed in [12] seems to be an adequate tool to describe the cluster structure when the optical system has a multiple aperture pupil.

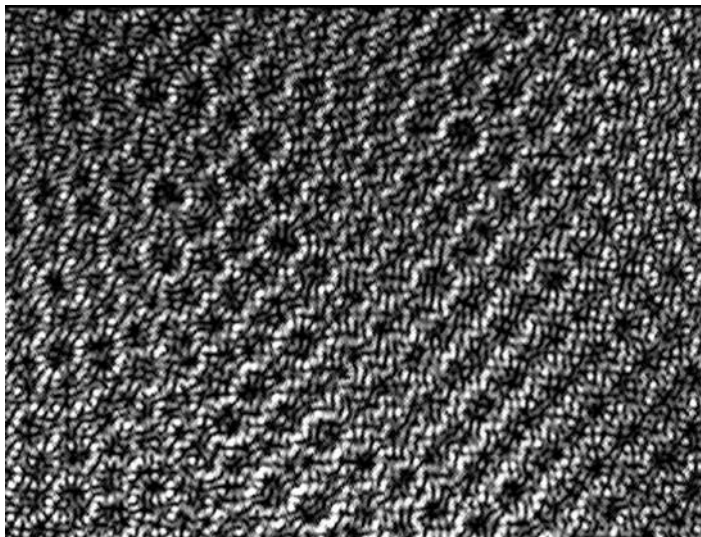


Figure 3. Experimental speckle pattern corresponding to 16 apertures uniformly distributed in a circumference.

In the following, we rewrite the main results of the mentioned model. This approach implies considering a pupil function formed by  $N$  non-overlapping apertures. The amplitude transmission function corresponding to the  $h$ th aperture is defined as  $a_h(u, v)$ . The field in the diffuser surface can be expressed as  $U_0(x, y) = \sum_{q=1}^m \tilde{U}_q(x, y) \exp(j\phi_q)$  which consists of a sum of  $m$  discrete scattering points with field amplitudes  $\tilde{U}_q(x, y)$  and phase  $\phi_q$  ( $j$  is the imaginary unit). Then, for  $N$  identical apertures of unitary transmission function with arbitrary distribution, the intensity distribution in the image plane ( $X - Y$  plane) results:

$$\begin{aligned}
I_i(X, Y) \propto & \left\{ \sum_{q=1}^m U_q^2 \left[ N + 2 \sum_{\substack{h, h'=1 \\ h > h'}}^N \cos(\phi_{qh} - \phi_{qh'} + \phi_h - \phi_{h'}) \right] + \right. \\
& + 2 \sum_{\substack{Pq, q'=1 \\ q > q'}}^m U_q U_{q'} \left[ \sum_{h=1}^N \cos(\phi_q - \phi_{q'} + \phi_{qh} - \phi_{q'h}) + \right. \\
& + \sum_{\substack{h, h'=1 \\ h > h'}}^N (\cos(\phi_q - \phi_{q'} + \phi_{qh} - \phi_{q'h'} + \phi_h - \phi_{h'})) \\
& \left. \left. + \cos(\phi_q - \phi_{q'} + \phi_{qh'} - \phi_{q'h} + \phi_{h'} - \phi_h) \right] \right\} \quad (1)
\end{aligned}$$

where

$$\phi_{qh} = -\frac{kr_h}{Z_0} (x_q \cos \alpha_h + y_q \sin \alpha_h) + \frac{k}{2Z_0} (x_q^2 + y_q^2),$$

$$\phi_h = -\frac{kr_h}{Z_C} (X \cos \alpha_h + Y \sin \alpha_h),$$

$$U_q(X, Y) = \iint dx dy \tilde{U}_q(x, y) A(x, y; X, Y),$$

$$A(x, y; X, Y) = \iint dudv a(u, v) \exp \left\{ jk \left[ u \left( \frac{x}{Z_0} + \frac{X}{Z_C} \right) + v \left( \frac{y}{Z_0} + \frac{Y}{Z_C} \right) \right] \right\},$$

$U_q(X, Y)$  is the amplitude in the image plane;  $A(x, y; X, Y)$  represents the response of the system to an impulsive input;  $k = \frac{2\pi}{\lambda}$ ;  $a(u, v)$  represents the amplitude transmission corresponding to an aperture;  $(x_q, y_q)$  is the random position of the  $q$ th scattering point of the diffuser;  $r_h$  is the distance from the geometrical centre of the  $h$ th aperture to the optical axis and  $\alpha_h$  is the angle that forms the segment  $r_h$  with the  $u$ -axis (see figure 1). Note that the first and second terms in equation (1) represent the superposition of intensities due to a single scattering point of the input diffuser. The third and fourth terms represent the contribution due to a pair of scattering points.

### 3.2 Auto-correlation of speckle intensity

In [11], it is stated that the speckle patterns obtained by using multiple aperture pupils fulfil the circular Gaussian random statistics with zero mean in the complex plane. This assertion is valid since the amplitude of the patterns results from the superposition of the complex amplitudes of light from the individual apertures satisfying the same statistics. Under this condition, by

following the same mathematical steps as in section 2.2 of [11] and starting from the autocorrelation function of the complex amplitude of the image field  $\langle U_q(X_1, Y_1)[U_q(X_2, Y_2)]^* \rangle$ , the auto-correlation function of the intensity distribution for a multiple aperture pupil arrangement results:

$$C_I(\Delta X, \Delta Y) = N^2 \langle I_0 \rangle^2 + |J_0(\Delta X, \Delta Y)|^2 \left[ N + 2 \sum_{\substack{h, h'=1 \\ h > h'}}^N \cos \{ \phi_h - \phi_{h'} \} \right], \quad (2)$$

where  $(\Delta X, \Delta Y) = (X_2 - X_1, Y_2 - Y_1)$ ,  $(X_i, Y_i)$  represents a point in the image plane,  $J_0(\Delta X, \Delta Y) \propto A(0, 0; \Delta X, \Delta Y)$  defines the correlation of the complex amplitude of waves propagating from an aperture to the points  $(X_1, Y_1)$  and  $(X_2, Y_2)$  in the image plane and  $\langle I_0 \rangle = J_0(0, 0)$ .

Equation (2) shows that the average transversal speckle dimensions are determined by the mean width of the function  $J_0(\Delta X, \Delta Y)$ , which depends only on the generic amplitude transmission function of the aperture  $a(u, v)$ , irrespective of the location of the apertures. Also, it could be inferred that the individual speckles are internally modulated by fringes. The expression inside the brackets in equation (2) determines the behaviour of the complex system of fringes that modulate the speckle due to the multiple interference of the wavefront coming from each aperture. Each pair of apertures  $a_h(u, v)$  and  $a_{h'}(u, v)$ , with  $h, h' = 1, 2, \dots, N$  and  $h \neq h'$ , can be associated with an elementary fringe system, specified by  $\cos\{\phi_h - \phi_{h'}\}$ .

Note that by considering a single scattering point on the optical axis in the input plane given by  $U_1(x, y) = \delta(x, y)$ , the intensity in the image plane is reduced to

$$I_i^{(m=1)}(X, Y) \propto A(0, 0; X, Y)^2 \left[ N + 2 \sum_{\substack{h, h'=1 \\ h > h'}}^N \cos(\phi_h - \phi_{h'}) \right]. \quad (3)$$

By comparing equations (2) and (3), the auto-correlation of intensity results

$$C_I(\Delta X, \Delta Y) = N^2 \langle I_0 \rangle^2 + K \cdot I_i^{(m=1)}(X, Y) \quad (4)$$

where  $K$  is a constant. Then, the intensity corresponding to a single scattering element is equivalent to the auto-correlation. Therefore, it can be advantageous to evaluate the output intensity of a single scattering to understand the result produced when a diffuser (multiple scattering elements) is employed in the input plane of the set-up.

#### 4. Results and discussion

The speckle cluster formation is analysed in terms of the parameters of the multiple aperture pupil to determine their influence in the cluster generation. The parameters to be considered are: the number of circular apertures  $N$ , the aperture radius  $R$ , the radius  $r$  of the circumference where the apertures are distributed and the uniformity of the aperture distribution in the mentioned curve. In our study, we concentrate on pupils with an even number of apertures due to their particularly high degree of symmetry.

As a first approach and by taking advantage of the assertion in the last paragraph of section 3.2, we analyse the cluster generation by considering the computed simulation of a single scattering element in the input plane and a multiple aperture pupil in front of the imaging lens. In this sense, figures 4, 5 and 6 show the theoretical intensity distribution in the image plane corresponding to a single scattering element obtained using equation (3). Taking into account

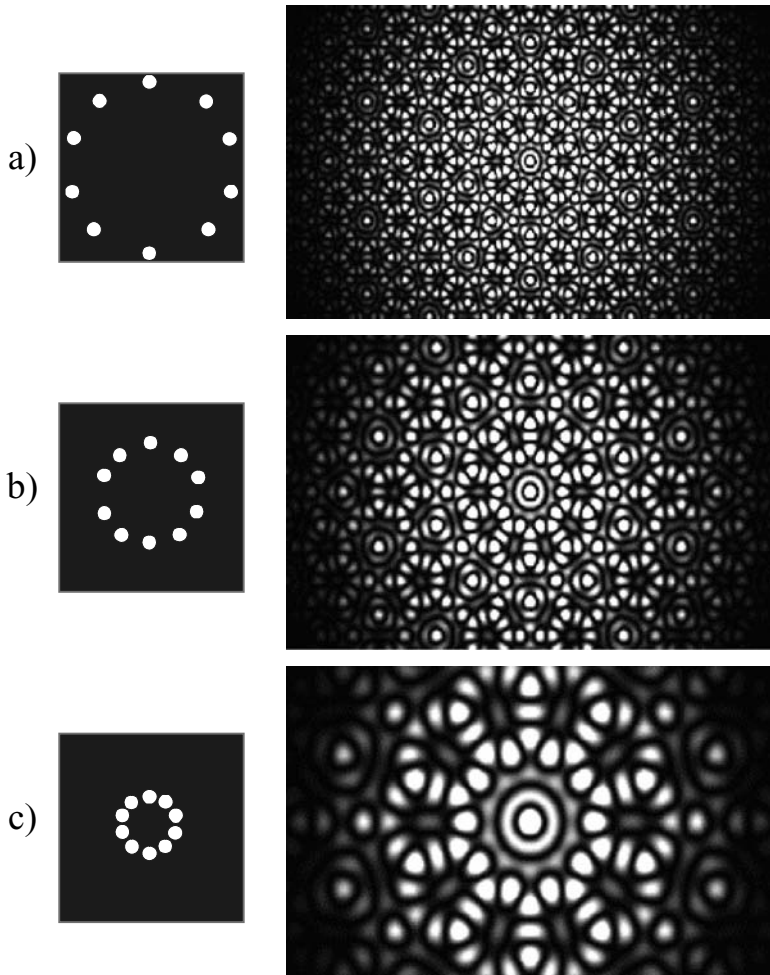


Figure 4. Simulations corresponding to a single scattering element for a pupil with 10 apertures ( $R = 0.4$  mm) uniformly distributed in a circumference of (a) radius  $r = 15$  mm, (b) radius  $r = 10$  mm and (c) radius  $r = 5$  mm. In each case the pupil is schematized.

that the apertures which form the pupil are circular, the resulting distributions are the well known Airy patterns modulated by a complex fringe system. The set of images in figures 4, 5 and 6 corresponds to simulated patterns where three parameters of the pupil keep fixed while the remaining parameter is changed.

The images in figure 4 correspond to a pupil with 10 apertures ( $R = 0.4$  mm), uniformly distributed in a circumference of radius: (a)  $r = 15$  mm, (b)  $r = 10$  mm and (c)  $r = 5$  mm. Note that in these images, the light intensity distribution in the pattern tends to concentrate in closed geometrical loci that replicate throughout the pattern. These replicated structures or unit cells are similar to that observed in the experimental result where a diffuser (multiple scattering elements) is utilized in the input plane (see figure 3). Then, this unit cell can be defined as a *regular cluster*. Note that the number of bright spots that form these cluster structures coincides with the number of apertures in the pupil. It is observed in figure 4 that the size of the unit cell changes in accordance with the circumference radius where the apertures are distributed. There is an inverse relation between the circumference radius and the dimensions of the cluster

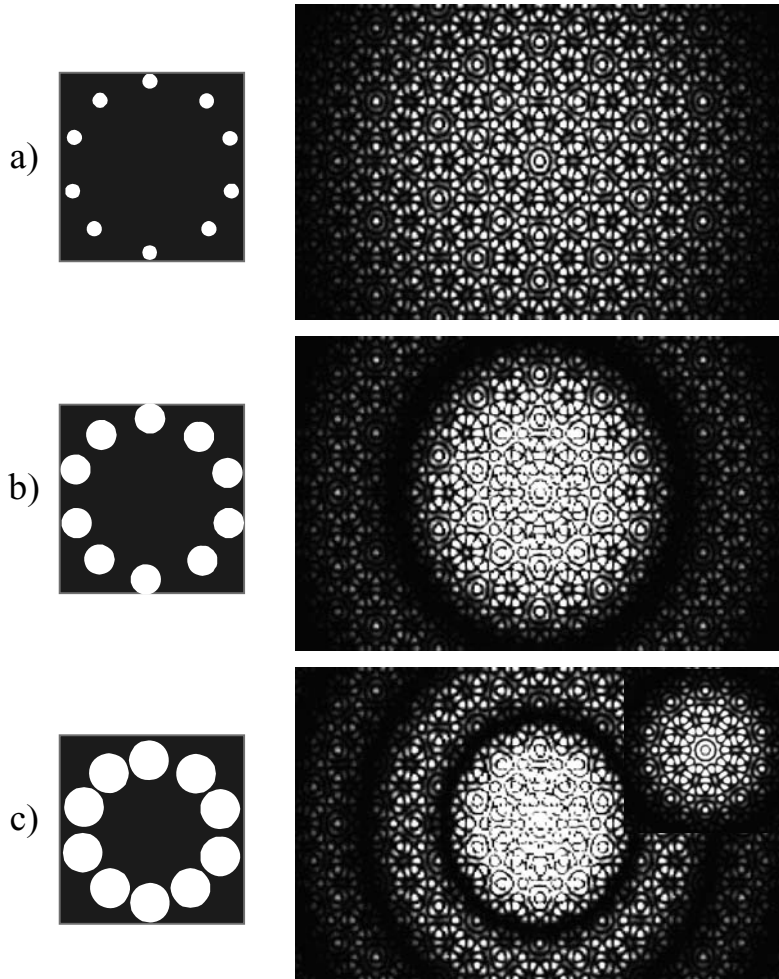


Figure 5. Simulations corresponding to a single scattering element for a pupil with 10 apertures uniformly distributed in a circumference of radius  $r = 15$  mm and (a) aperture radius  $R = 0.4$  mm, (b) aperture radius  $R = 0.8$  mm and (c) aperture radius  $R = 1.2$  mm. In each case the pupil is schematized. The insert in (c) shows a non-saturated version of the central region of the diffraction Airy pattern.

that replicates in the pattern. When the circumference radius increases, the apertures part from each other and the elementary fringe systems that modulate the pattern increase in frequency without changing their directions.

The computer simulations in figure 5 are obtained by using a pupil with 10 apertures uniformly distributed in a circumference ( $r = 15$  mm) and apertures with radius: (a)  $R = 0.4$  mm, (b)  $R = 0.8$  mm and (c)  $R = 1.2$  mm. It is apparent that when the radius of the apertures increases, the Airy pattern decreases accordingly. However, the set of elementary fringes that modulates the pattern remains constant. This effect occurs because the number of apertures and the radius of the circumference where the apertures are uniformly distributed do not change. Then, the regular cluster maintains its size and shape in all cases. In summary, the cluster structure is governed by the inner speckle modulation and does not depend on the aperture dimensions. Indeed, as the aperture radius increases, the energy distribution in the Airy pattern changes so that the central disk of the diffraction pattern reduces its size and



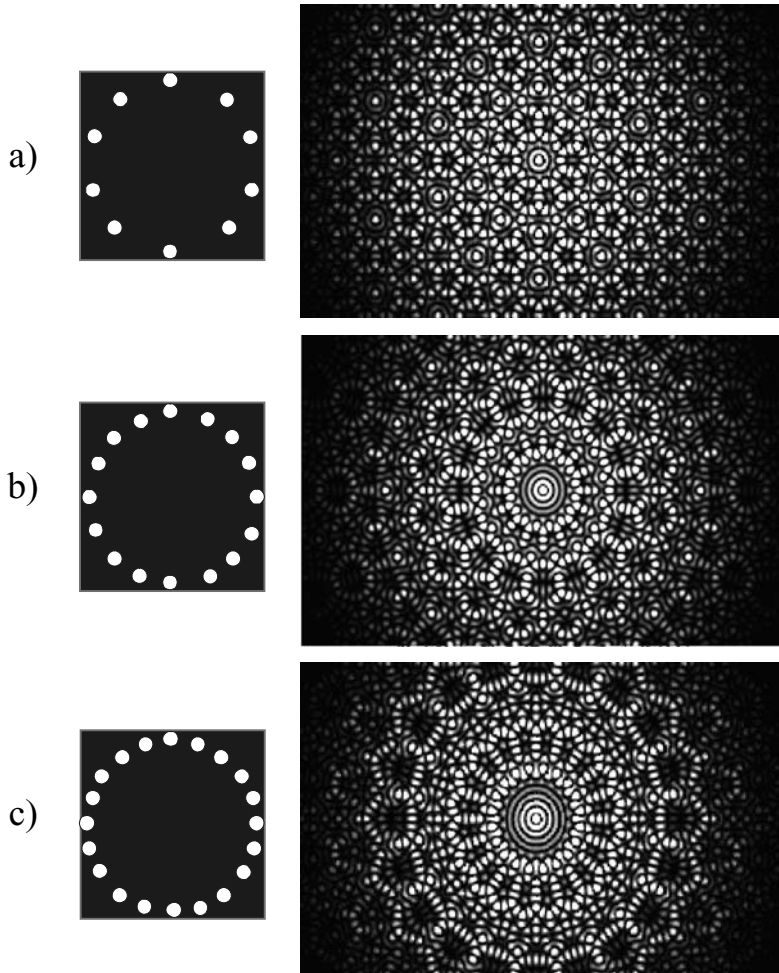


Figure 6. Simulations corresponding to a single scattering element for:  $r = 15$  mm,  $R = 0.4$  mm and a pupil with (a) 10 apertures, (b) 16 apertures and (c) 20 apertures. In each case the pupil is schematized.

increases its relative intensity. Note that the central region of the pattern in figure 5(c) is saturated. However, the cluster structure remains in the whole pattern and in particular in the central region as confirmed by observing the non-saturated version of the central region of the pattern (see the inset in figure 5(c)).

Figure 6 also considers a single scattering element corresponding to a pupil with: (a) 10 apertures, (b) 16 apertures and (c) 20 apertures (radius  $R = 0.4$  mm), uniformly distributed in a circumference of ratio  $r = 15$  mm. Note that, the regular cluster in its first appearance around the centre of the pattern lies replicated on a circumference with a multiplicity that coincides with the number of apertures. In addition, the regular cluster size increases proportionally with the number of apertures. Both effects mean that the regular cluster formation increasingly departs from the pattern centre (see the sequence in figure 6). For instance, in the 20-aperture case the regular clusters are observed in the rim of the central Airy disk. On the other hand, in the 10-aperture case, the regular clusters appear closer to the central region of the diffraction pattern and the resulting distribution presents a higher cluster, repetitively.

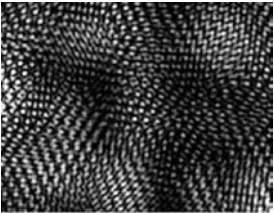
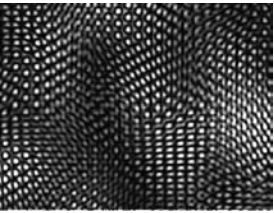
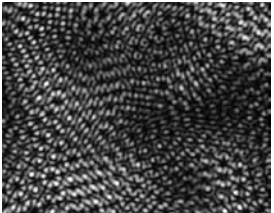
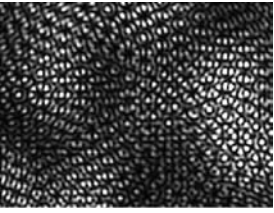
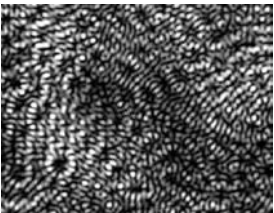
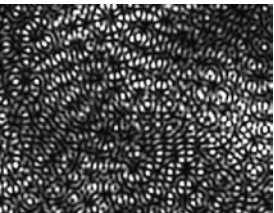

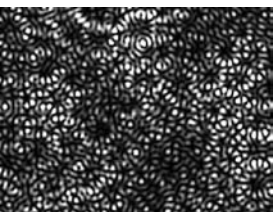
	Experimental speckle pattern	Simulated speckle pattern
a)		
b)		
c)		
d)		

Figure 7. Experimental and simulated speckle pattern corresponding to a pupil with (a) 6 apertures, (b) 8 apertures, (c) 12 apertures and (d) 16 apertures uniformly distributed in a circumference of radius  $r = 15$  mm (aperture radius  $R = 1.3$  mm). In each case the pupil is schematized.

The previous results permit the characterization of the cluster formation when there is only a single scattering element in the input. However, our interest corresponds to using a diffuser element in the input plane, which implies a huge amount of scattering elements. Nonetheless, as mentioned above, the response based on a single scattering element is useful for understanding the behaviour of the resulting pattern when multiple scattering elements are used. The experimental and simulated images in figure 7 correspond to the use of several scattering elements in the input plane. The sequence shows speckle patterns obtained with an increasing number of apertures uniformly distributed in the pupils but maintaining a fixed aperture diameter and circumference radius. The agreement between the theoretical and experimental results should be emphasized. As predicted by our previous analysis corresponding to a single scattering element, figure 7 shows that the average speckle size is independent of the number of apertures lying on the circumference. This feature is apparent in figure 7(a) and (b). In

figure 7(c) and (d) the speckle structure is not evident because the inner modulations dominate the pattern.

The results of figure 7 confirm that the light intensity distribution in the pattern tends to concentrate in geometrical loci (*regular cluster*). In the 6-aperture case a regular distribution of six bright spots that resemble the aperture arrangement in the pupil become apparent (see figure 7(a)). In fact, the number of spots that form the regular cluster increases in the same proportion as the number of apertures. Furthermore as far as the number of apertures increases the regular cluster radius becomes greater.

The 16-aperture case (figure 7(d)) shows that the cluster structure loses its regularity. This effect can be understood by remembering the results obtained for a single scattering element. In figure 6 for 20 apertures the regular cluster first appears in the rim of the central Airy disk. Note there is an increase in the aperture radius between figures 6 and 7. In the case that the pattern corresponding to a single scattering element is analysed, a decrease in the Airy disk is observed in comparison with figure 6. Then, the regular cluster in the 16-aperture case first appears in the inner ring of the diffraction pattern. This effect implies that the cluster structure decreases its regularity in the case of multiple scattering elements. Note that according to the previous discussion, if the number of apertures as well as the radius of the circumference where they are distributed are kept constant, then the cluster regular structure could be recovered by reducing the aperture radius.

Figure 8 shows experimental and simulated results for 16 apertures with  $R = 0.5$  mm distributed uniformly over circumferences of: (a) radius 15 mm and (b) radius 10 mm. By observing figure 8 some features of the cluster structure can be withdrawn. At this point, the possibility of controlling the appearance of the regular cluster by changing the pupil geometrical parameters is apparent. A comparison between figures 7(d) and 8(a) demonstrate that a decrease in the aperture radius whilst maintaining the other pupil geometrical parameters constant, allows the appearance of regular cluster structures. As stated above, in figure 5 in the

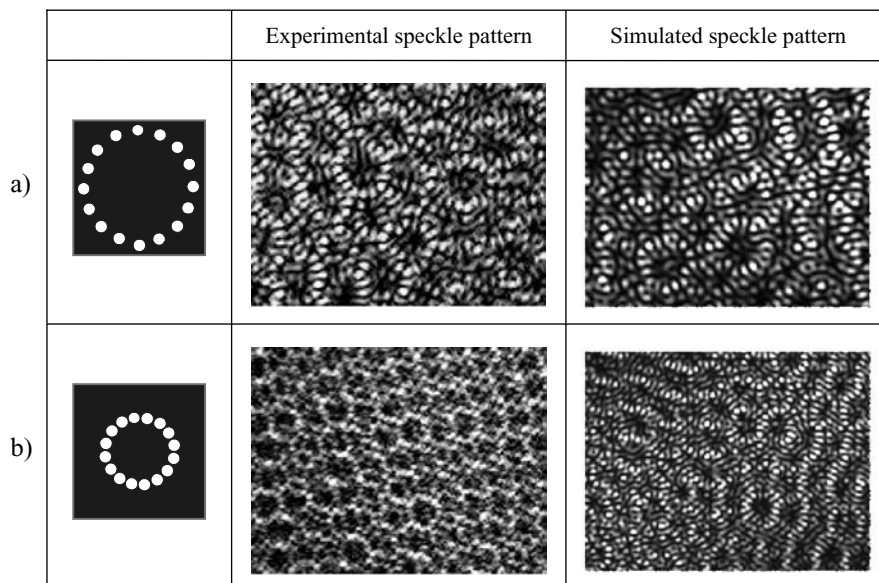


Figure 8. Experimental and simulated speckle pattern corresponding to a pupil with 16 apertures uniformly distributed in a circumference of (a) radius  $r = 15$  mm, (b) radius  $r = 10$  mm (aperture radius  $R = 0.5$  mm). In each case the pupil is schematized.

case of a single scattering element, a decrease in the aperture radius increases the central Airy disk size but without changing the elementary fringe systems. Therefore, in this case more cluster structures appear in the central Airy disk, which implies in the multiple scattering elements case an increase in the regularity of the observed pattern (see figure 8). Indeed, it is apparent from figure 8 that the regular cluster radius is inversely proportional to the circumference radius where the apertures are distributed. This result is in accordance with the discussion in figure 4.

The previous analysis determines the conditions for obtaining a regular cluster when the apertures that form the pupils are uniformly distributed in a circumference. However, it is interesting to analyse the effect of the uniformity in the cluster formation. Then, we consider a more general arrangement: multiple apertures non-uniformly distributed on a circumference. Figure 9 shows simulated patterns for 10 apertures uniformly and non-uniformly distributed on a circumference. To understand the speckle distribution behaviour corresponding to a multiple scattering element (figure 9(c) and (d)), a single scattering element situation is depicted (figure 9(a) and (b)). It is apparent that in the non-uniform case, the regularity of the cluster structure diminishes (figure 9(b) and (d)). The pattern loses the multiplicity of redundant elementary fringe systems that reinforce the regularity and, in turn, new isolated elementary fringe systems contribute, producing the mentioned diminishing of the cluster regularity.

To resume, it is useful to remember that in the case of ring-slit aperture pupils the autocorrelation function of the speckle exhibits long ringing lobes bringing a long-range interaction

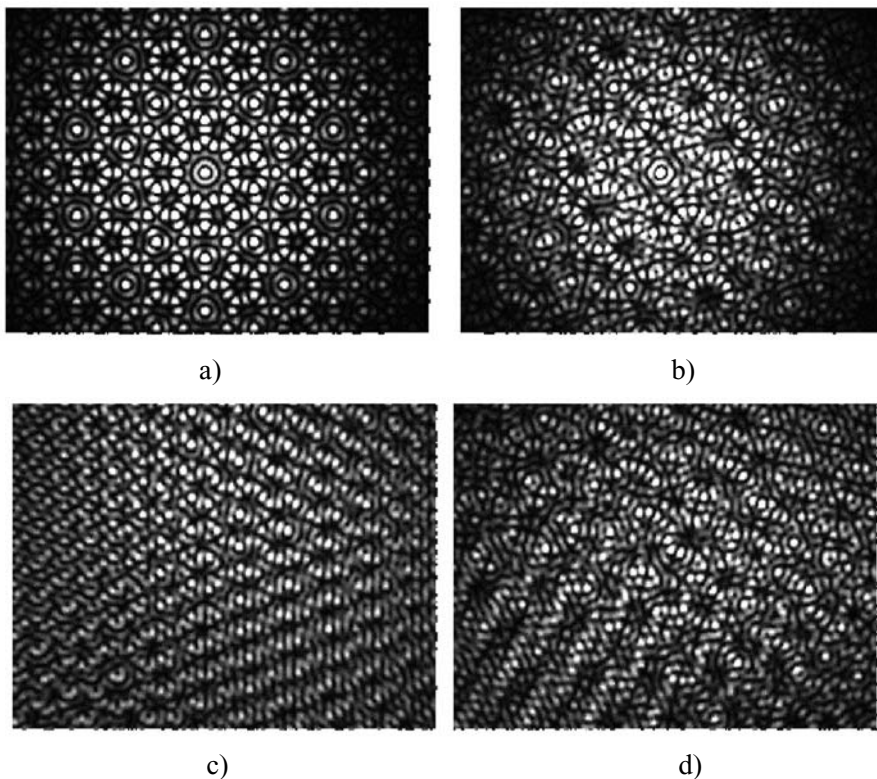


Figure 9. Simulated speckle pattern corresponding to a pupil with 10 apertures distributed in a circumference ( $r = 15$  mm,  $R = 0.5$  mm) with (a) a single scattering element in the input and uniformly distributed apertures; (b) a single scattering element and non-uniformly distributed apertures; (c) a multiple scattering element and uniformly distributed apertures and (d) a multiple scattering element and non-uniformly distributed apertures.

among the speckles [3]. As stated above, the ring-slit aperture pupil is a limiting case of the discrete aperture arrangement. Then, it is clear that when passing from one to several apertures in the pupil mask the autocorrelation function gradually begins to form the long ringing lobes. As demonstrated above, this fact is a consequence of the appearance of more elementary fringe systems, which depend on the aperture numbers and the curve in which they are distributed. Moreover, it is possible to control the autocorrelation in order to include or not include regular clusters in the central Airy disk. Therefore, the possibility of determining conditions that depend on the pupil parameters selection in order to obtain regular cluster with a 'better definition' is apparent (see results in figure 8).

Previously, we proposed several applications using photorefractive materials in the recording of speckle distributions, where multiple aperture pupil optical systems are involved [13]. Moreover, as analysed in [14, 15], optical vortices (wave front dislocations) appear in speckle distributions. Hence, the appearance of these wave front dislocations in modulated speckle could be inferred. Finally, if there is interest in applications that involve cluster non-linear recording a deeper cluster behaviour analysis that considers optical vortices could be done.

## 5. Conclusions

A ground glass acting as a multiple scattering element generates a speckle pattern. In our work, we analyse the high cluster regularity presented in the image speckle pattern when using an arrangement of apertures attached to the imaging lens. We also demonstrate that the intensity corresponding to a single scattering element is equivalent to the auto-correlation. This result is the key point in order to interpret the speckle cluster formation.

When a single scattering element is considered, we demonstrate that the regular cluster is governed by the number and radius of the apertures, the uniformity of the distribution of the apertures and the radius of the circumference where the apertures are distributed. In particular, when an even number of apertures uniformly distributed in a circumference is considered, it is observed that the cluster replicates the aperture array. It means that the tiny spots forming the regular cluster are arranged as a scaled version of the distribution of the apertures in the pupil. Also, the cluster radius is proportional to the number of apertures and is inversely proportional to the circumference radius. Besides, the cluster size does not depend on the aperture radius. However, a decrease in the aperture radius produces an increase in the size of the Airy disk, allowing thereby the appearance of more and more regular cluster structures when a single scattering element is considered. These features allow a 'better defined' regular speckle cluster in the multiple scatterings element case to be generated.

Besides, we analyse the effect on the speckle cluster, when the apertures are non-uniformly distributed in the closed curve (circumference). In this case, we demonstrate that the regularity of the speckle cluster structure is broken. This effect appears as a consequence of the loss of elementary fringe systems that reinforce the regularity in the uniform case and the appearance of new isolated elementary fringe systems without symmetrical counterparts.

Finally, it should be mentioned that the regular cluster appears not only when the closed curve is a circumference. Therefore, further analysis related to the inclusion of more general geometries in the closed curves should be considered.

This experiment allows regular intensity arrangements from random procedures to be obtained. These sub-speckle structures imply a reduction in the average speckle size by more than one order of magnitude. It means that the speckle patterns result in a highly localized spot structure. These features suggest the possibility of implementing light particle steering where the regular cluster pattern provides an optical tweezer tool.

## Acknowledgments

This research was performed under the auspices of CONICET PIP 5995 (Argentina), CICIPBA (Argentina), ANPCYT PICT 12564 (Argentina) and Facultad Ingeniería, Universidad Nacional de La Plata (Argentina).

## References

- [1] Erf, R. K., 1978, *Speckle Metrology* (New York: Academic Press).
- [2] Dainty, J. C. (Ed.), 1975, *Laser Speckle and Related Phenomena* (Berlin: Springer-Verlag).
- [3] Angel, L., Tebaldi, M., Trivi, M., and Bolognini, N., 1999, Optical operations based on speckle modulation by using a photorefractive crystal. *Optics Communication*, **168**, 55–64.
- [4] Angel Toro, L., Tebaldi, M., Bolognini, N., and Trivi, M., 2000, Speckle photography with different pupils in a multiple exposure scheme. *Journal of Optical Society of America A*, **17**, 107–119.
- [5] Tebaldi, M., Angel Toro, L., Trivi, M., and Bolognini, N., 2000, New multiple aperture arrangements for speckle photography. *Optics Communications*, **182**, 95–105.
- [6] Angel, L., Tebaldi, M., Trivi, M., and Bolognini, N., 2002, Phase object analysis with a speckle interferometer. *Optics Letters*, **27**, 506–508.
- [7] Tebaldi, M., Angel, L., Trivi, M., and Bolognini, N., 2003, Phase-object detection by use of a double-exposure fringe modulated speckle patterns. *Journal of Optical Society of America A*, **20**, 116–129.
- [8] Tebaldi, M., Ángel, L., Bolognini, N., and Trivi, M., 2004, Speckle interferometric technique to assess soap films. *Optics Communications*, **229**, 29–37.
- [9] Uno, K., Uozumi, J., Asakura, T., 1995, Speckle clustering in diffraction patterns of random objects under ring-slit illumination. *Optics Communications*, **114**, 203–210.
- [10] Ibrahim, M., Uozumi, J., and Asakura, T., 1997, On the generation of clustered speckles due to ring-slit illumination. *Optik*, **106**, 33–41.
- [11] Angel, L., Tebaldi, M., Trivi, M., Bolognini, N., 2001, Properties of speckle patterns generated through multiaperture pupils. *Optics Communications*, **192**, 37–47.
- [12] Lencina, A., Vaveliuk, P., Tebaldi, M., and Bolognini, N., 2003, Modulated speckle simulations based on the Random-walk model. *Optics Letters*, **28**, 1748–1750.
- [13] Barrera, J. F., Henao, R., Tebaldi, M., Bolognini, N., and Torroba, R., 2006, Multiple image encryption using an aperture-modulated optical system. *Optics Communications*, **261**, 29–33.
- [14] Zel'dovich, B. Ya., Pilipetsky, N. F., and Shkunov, V. V., 1985, Properties of speckle-inhomogeneous fields. In *Principle of Phase Conjugation* (Berlin: Springer-Verlag).
- [15] Baranova, N. B., Zel'dovich, B. Ya., Mamaev, A. N., Pilipetsky, N. F., and Shkunov, V. V., 1983, Wave front dislocations: topological limitations for adaptive systems with phase conjugation. *Journal of Optical Society of America*, **73**, 525–528.